Accelerated and Efficient Photochemistry from Higher Excited Electronic States in Fulgide Molecules

8 **AUTHORS**, INCLUDING:

Artur Nenov
University of Bologna

26 PUBLICATIONS **172** CITATIONS

Accelerated and Efficient Photochemistry from Higher Excited Electronic States in Fulgide Molecules

Thorben Cordes,[†,‡] **Stephan Malkmus,**[†,‡] **Jessica A. DiGirolamo,**[§] **Watson J. Lees,**[§] **Artur Nenov,**[∥] **Regina de Vivie-Riedle,**[∥] **Markus Braun,**[†,‡] **and Wolfgang Zinth**[*,†,‡]

Lehrstuhl für BioMolekulare Optik, Department Physik, Ludwig-Maximilians-Universität München, Oettingenstrasse 67, D-80538 München, Germany, Munich Center for Integrated Protein Science CIPS^M, Department of Chemistry and Biochemistry, Florida International University, 11200 SW Eighth Street, Miami, Florida, 33199, and Department Chemie and Biochemie Ludwig-Maximilians-Universität München, Butenandtstrasse 11, 81377 München, Germany

Received: August 8, 2008; Revised Manuscript Received: September 29, 2008

The photoinduced electrocyclic ring-opening of a fluorinated indolylfulgide is investigated by stationary and ultrafast spectroscopy in the UV/vis spectral range. Photoreactions, initiated by optical excitation into the S_1 (570 nm) and S_N (340 nm) absorption band of the closed isomer, lead to considerable differences in reaction dynamics and quantum yields. Transient absorption studies point to different reaction pathways depending on the specific excitation wavelength: excitation into the S_1 state leads to the known reaction behavior with a picosecond decay to the ground state and a small quantum yield of 7% for the photoproduct. The S_N state shows an unexpected long lifetime of 0.5 ps. The photoreaction starting from the S_N state leads to a large extent directly to the product ground state and back to the educt ground state. This results in an increased reaction quantum yield of 28%. In contradiction to Kasha's rule, the S_1 state is only populated with an efficiency of 38%. The observed behavior strongly differs from the expected picture with fast relaxation into the S_1 state and a subsequent ring-opening reaction starting from the lowest excited electronic state. Quantum chemical calculations confirm and complement the experimental findings allowing a sound molecular interpretation to be obtained.

Introduction

It is generally accepted that luminescence phenomena in solution-phase chemistry occur from vibrationally relaxed molecules in their lowest excited singlet (S_1) or triplet (T_1) states. These observations have been condensed in the Kasha and Kasha–Vavilov rule. Here, it is stated that the emission of a molecule in solution originates from the lowest excited state independently of the state which is initially excited (Kasha rule[1]). Moreover, the fluorescence quantum yield is found to be constant irrespective of the photoexcitation wavelength (Kasha–Vavilov rule[2]). An equivalent rule for photochemical reactions has not been formulated, but many investigations corroborate the same mechanistic picture also for photochemical processes.[2,3]

The rules are related to the observation that relaxation in the condensed phase from higher electronically excited states S_N into the lowest excited state of the same manifold is generally much faster than the direct decay of a state S_N into the ground-state S_0 or other reaction channels like intersystem crossing (ISC), fluorescence emission, or photochemical reactions. Theoretically, the rate of internal conversion (IC) from the zero vibrational level of an upper excited state (e.g., S_2) into the S_1 state may be described in terms of the energy-gap law.[4] Here, the rate is determined by the Franck–Condon factor and the coupling element between the two involved electronic states.[2,5]

The relatively small energetic distance between excited electronic states and the manifold of vibrational modes lead to very large values of these IC rate constants up to 1×10^{14} s^{-1}. These extremely high rate constants are often contributed to the involvement of conical intersections.[6] Kasha's rule cannot be applied to the gaseous phase, where collisions are rare and energy dissipation is slow. In the case of gaseous thiophosgene, fluorescence from S_2 with a quantum yield near unity can be observed.[7,8] However, even in condensed phase, experimental deviations were found and point to very unique, often unexpected, molecular properties.[2] Anomalous fluorescence from higher excited electronic states in solution has been observed for azulene and several of its benzene-annulated derivatives.[9,10] For photochemical reactions, anomalous behavior has been reported for azobenzene[11] and after multiphoton-excitation processes in diarylethene and fulgide systems where high-lying and extremely reactive states are populated.[12]

Deviations from the rules appear when IC processes out of a specific excited electronic state to the lowest excited state are unusually slow, when the photochemical reaction rates out of the higher excited states are extremely fast, or when the lowest excited electronic state has an unexpected short lifetime. In this respect, it is of great interest to understand why some higher electronic states are so long-lived that other reaction channels may compete with internal conversion to S_1. The reasons for deviations from Kasha's rule in solution-phase photochemistry are often difficult to obtain. As described above, the Franck–Condon factor and the coupling elements between the two states mainly determine the rate of internal conversion from S_2 to S_1. The rate is hence reduced if one (or both) of the factors for internal conversion is small. However, it is sometimes chal-

* To whom correspondence should be addressed. Fax: (+49) 89-2180-9202. E-mail: zinth@physik.uni-muenchen.de.
† Department Physik, Ludwig-Maximilians-Universität München.
‡ Munich Center for Integrated Protein Science CIPS^M.
§ Florida International University.
∥ Department Chemie and Biochemie Ludwig-Maximilians-Universität München.

Photochemistry in Fulgide Molecules

J. Phys. Chem. A, Vol. 112, No. 51, 2008 **13365**

SCHEME 1: Structure and Schematic Drawing of the Ring-Opening Reaction of the Investigated Indolylfulgide[a]
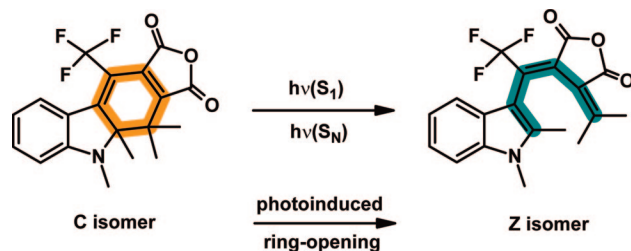
[a] The reaction can be initiated by both S_1 and S_N excitation of the *C*-isomer (left).

lenging to distinguish between the case of a poor Franck−Condon factor, meaning that the energy gap between the two states is large, or a small coupling element which may result when the wave functions of the two states are essentially orthogonal. It is known for the well-studied azulene that the long lifetime of the S_2 state arises from a small Franck−Condon factor for the internal conversion process from S_2 to S_1 which reduces the internal conversion rate for the S_2 to S_1 process down to 7×10^8 s^{-1}.[13] Simultaneously, accessible conical intersections between S_1 and S_0 are responsible for the observed ultrafast decay of the S_1 state.[14,15]

It is the aim of this paper to present a photochemical reaction in solution which directly occurs from higher excited states S_N. The paper addresses an excitation-wavelength-dependent ring-opening reaction of a trifluoromethyl-substituted fulgide. It will be shown using stationary absorption experiments that the photochemical quantum yield of the ring-opening reaction is increased by a factor of ∼4 when actinic light in the near UV (excitation into higher electronic states S_N) is used instead of visible light (excitation to the lowest singlet-state S_1). Details of the photoreaction dynamics induced by the different excitation wavelengths are obtained using femtosecond transient absorption spectroscopy (TA) in the visible range. The studied ring-opening reaction reveals completely different transient absorption dynamics upon S_1 (570 nm) and S_N (340 nm) excitation. The observed transients suggest a reaction model with a slow internal conversion between the excited S_N and the S_1 state and a fast direct reaction pathway to the ground state of educt (*C*-isomer) and product (*Z*-isomer). The present study demonstrates photochemistry of higher excited states observed in real time with femtosecond time resolution. Quantum chemical calculations support the experimental findings and contribute to the detailed understanding of the involved molecular processes.

Material and Methods

Experimental Details. The trifluoromethyl-substituted indolylfulgide (structure see Scheme 1) was synthesized by a procedure published elsewhere.[16] The compound was dissolved in cyclohexane (Merck, purity 99% used as purchased without further purifications). During the time-resolved measurements, the sample was kept in a defined photostationary state (PSS400, >90% *C*-isomer) with high concentrations of the investigated *C*-isomer. PSS400 was generated by illuminating the sample with UV light around 400/430 nm (Hg/Xe lamp, Hamamatsu, filtered by GG385 (3 mm) and BG1 (1 mm), Schott). Meanwhile, the sample solution was pumped through a flow cuvette (fused silica windows, optical path length 0.5 mm) by a peristaltic pump to ascertain the defined starting condition.

A spectrophotometer (Perkin-Elmer, Lambda 19) was used to measure the stationary UV/vis absorption spectra. The

quantum yields of the ring-opening reaction were determined by illumination into the S_1 and the S_N absorption bands of a sample containing exclusively the *C*-isomer. In these experiments, changes in sample composition induced by the actinic light within a certain time period were determined from the absorption change ΔOD in a characteristic band. The following light sources were used for illumination: Light at a wavelength of 532 nm (S_1 excitation) was obtained from a frequency-doubled Nd:YAG laser (Laser Compact Plus Co. Ltd., type LCM-T-111, Russia). A Hamamatsu Hg/Xe lamp (Hamamatsu, Lightningcure LC4, Japan) combined with suitable filtering (WG350, 3 mm and UG5, 1 mm, Schott) was used as UV source at 365 nm (S_N excitation). A detailed procedure for the determination of the photochemical quantum yield is found in ref 17.

Femtosecond pump−probe spectroscopy in the visible and near-ultraviolet spectral range was used to investigate the dynamics of photochemical reactions for different excitation conditions. A home-built Ti:Sa based regenerative amplifier laser system generated ultrashort pump and probe pulses (for details of the system, see refs 17−20). Tunable pump pulses in the visible spectral range were generated in a noncollinear optical parametric amplifier (NOPA).[21,22] The NOPA was adjusted to produce light pulses at 680 and 570 nm. For excitation in the visible, the NOPA pulses at 570 nm were compressed to ∼100 fs using a prism setup. The UV excitation pulses centered at 340 nm were obtained by frequency doubling the 680 nm pulses from the NOPA in a 100 μm BBO crystal (type I). Excitation energies varied from 250 to 500 nJ. A femtosecond white light continuum generated in CaF$_2$ was used as probe pulse (380−650 nm).[23] Transient absorption changes in the white light continuum were recorded at various delay times between pump and probe pulse using a multichannel detection setup.[24] For pump pulses at 570 nm, scattering of excitation light influences probing in the wavelength region from ∼560 to 580 nm. The instrumental response time (full width at half-maximum (fwhm)) for excitation in the UV range was determined to be ∼250 fs. A better time resolution (∼100 fs) was achieved for pump pulses at 570 nm. The spot diameter of the pump light was in the range of ∼120 μm providing a homogeneous excitation density for the probe−pulse (diameter ∼40−50 μm). The polarization of pump and probe pulses at the sample location was at magic angle. A global fit analysis based on a Levenberg−Marquart algorithm was used to extract decay associated spectra from the transient absorption data set.[25]

Theoretical Details. The search for conical intersections between the S_1 and S_0 states of the indolylfulgide was performed in full dimensions on the CASSCF-level with GAUSSIAN03.[26] We used a manually generated basis set. For optimal description of the photoactive part, the central C6-ring (Scheme 1) with its three attached methyl groups and one trifluoromethyl group was treated with a 6−31G* basis set, which we also selected for the adjacent N atom. All other atoms were treated with a 6−31G basis set. The CASSCF calculations were performed with six active electrons in six orbitals. The active space was chosen in order to include the π-type molecular orbitals on the central C6-ring, where the photoexcitation occurs. The σ-bond, which is broken or formed during the photochemical process, was also included. Further details can be found in the Supporting Information.

Results

Steady-State Experiments. The two involved isomers of the fluorinated fulgide, namely, the open *Z*-form and the closed
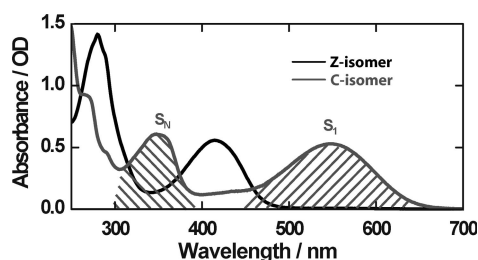
Figure 1. Absorption spectra of both *C*/*Z*-isomers of the indolylfulgide in cyclohexane. The gray line corresponds to the *C*-isomer; different absorption bands of the *C*-isomer (S_1/S_N) are marked. The absorption spectrum of the *Z*-isomer is shown in black.

C-form, are drawn in Scheme 1. Stationary absorption spectra of the respective molecular forms are shown in Figure 1 for the open *Z*- (black line) and the closed *C*-forms (gray line). Both absorption spectra feature distinct absorption bands.

For the *C*-form, they are tentatively assigned to the S_1 state (Figure 1, gray, around 550 nm) and the S_N state (Figure 1, gray, around 350 nm). Since quantum chemical calculations place different excited electronic states (S_2, S_3, S_4) in the wavelength region around 350 nm, a more general identifier S_N is used for this transition, which stands for a superposition of states reached by optical excitation at 340 nm.

The S_1 state of the *Z*-form absorbs around 420 nm. Transitions corresponding to higher electronic excitations are found at wavelengths <340 nm (Figure 1, black).

The *Z*-isomer and the *C*-form interconvert by illumination into the respective absorption bands (Figure 1). Since *Z*- and *C*-isomer absorption spectra show only little overlap, both molecular forms can be prepared in high concentrations applying adequate illumination. High concentrations of the *C*-isomer in TA investigated samples in combination with the low extinction coefficient of the *Z*-isomer at the excitation wavelengths 340/570 nm (Figure 1) assure that the experimental TA data exclusively represent photoreactions of the *C*-isomer. Also, the *E*-isomer may be generated with small efficiency after photoexcitation of the *Z*-isomer at 270/400 nm. Under the experimental conditions of the presented experiments, the influence of the *E*-isomer can be excluded because of the following arguments: (1) Care was taken to use a sample with high concentrations of the *C*-isomer with only minor concentrations of the E-isomer. (2) The *E*-form has smaller absorption cross sections than the *C*-form at the used excitation wavelengths, and (3) no formation of the *E*-isomer directly from the *C*-form has been reported.[27]

The reaction quantum yield of the ring-opening reaction after excitation into the S_1 and S_N absorption bands (see Figure 1) at 532 nm (S_1) and 365 nm (S_N) was determined using purified samples containing only the *C*-form of the fluorinated indolyl-fulgide. The results are summarized in Table 1. A strong difference of the photochemical quantum yields is found for the two excitation wavelengths. Concerning the excitation into the S_1 state, a value of QY(S_1, *C*→*Z*) = 7($\pm$1)% is obtained.

Excitation of the S_N state leads to a 4-fold increase in quantum yield of QY(S_N, *C*→*Z*) = 28($\pm$2)%.

Time-Resolved Measurements. Detailed information on the molecular background of the excitation-dependent quantum yield is obtained using time-resolved absorption spectroscopy. We investigated the *C*→*Z* photoreaction by exciting the indolyl-fulgide molecules in the state PSS400 with femtosecond pulses at two wavelengths: 570 nm for S_0 to S_1 excitation and 340 nm for the excitation into the S_N state. The absorption changes representing the reaction dynamics are recorded with suitably delayed broad band probe pulses between 380 and 650 nm. Figure 2 gives an overview of the transient absorption data obtained with the different excitation wavelengths.
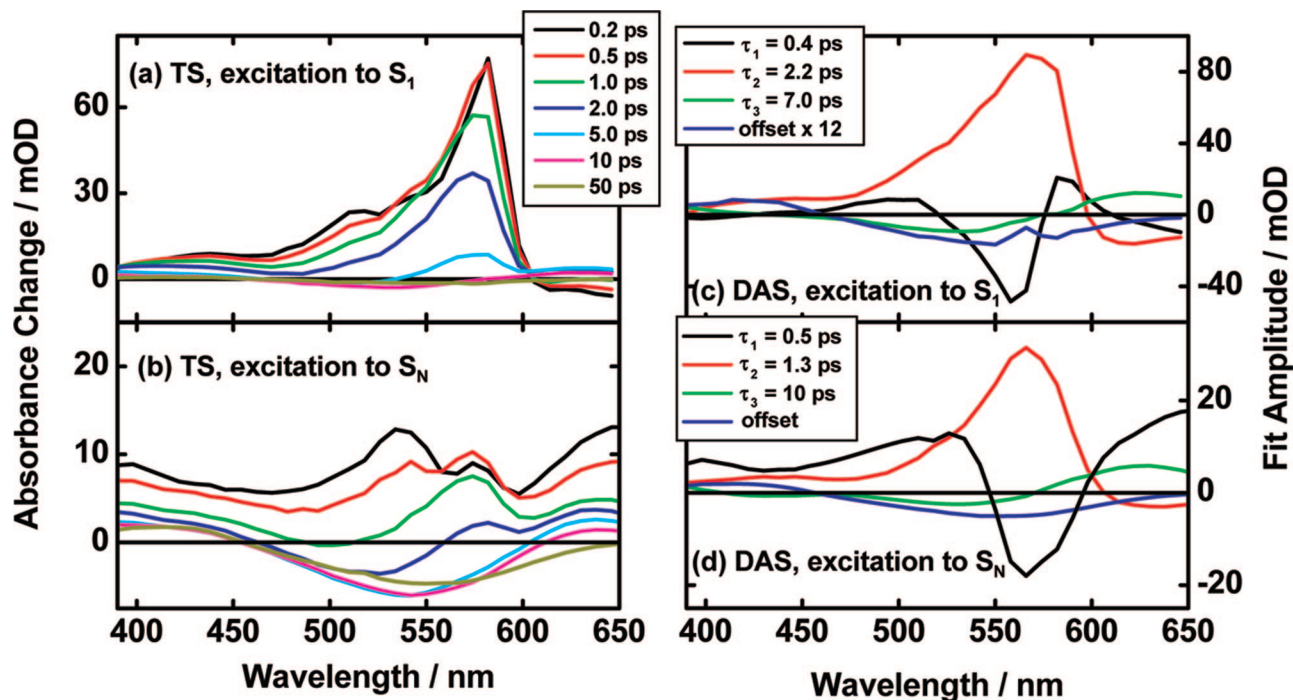
***C*→*Z* Reaction via S_1 Excitation.** Immediately after the absorption of the 570 nm pulse, an induced absorption band can be observed (Figure 2a, t_D = 0.2 ps), which extends from the near UV until 600 nm featuring a pronounced peak at 580 nm with intense absorbance. Negative signal contributions are found at longer probing wavelengths λ_{pr} > 610 nm. Both features can be assigned to the population of the excited electronic state S_1, which leads to (1) excited-state absorption (ESA), dominating at λ_{pr} < 600 nm, (2) the bleaching of the ground-state absorption band, which modulates ESA, and (3) stimulated emission (SE) seen as a negative signal at wavelengths λ_{pr} > 610 nm. In the early time regime, wave-packet-like oscillatory features (data not shown) are seen up to t_D $\sim$ 0.6 ps in the wavelength region from 580 to 650 nm. During this time period, only weak variations of the spectrum occur (Figure 2a, t_D = 0.2 ps, 0.5 ps). Subsequently, the absorption change decays on the time scale of a few picoseconds (Figure 2a, t_D = 0.5 ps, 1.0 ps, 2.0 ps). After these dominant kinetics, a spectrum with negative signal around 530 nm and positive signal >600 nm remains, which decays into a constant offset spectrum on a time scale of 10 ps (Figure 2a, t_D = 5.0 ps, 10 ps, 50 ps). The constant difference spectrum found at delay times t_D > 50 ps resembles the stationary absorption difference spectrum found in steady-state experiments: increased absorption in the low wavelength region ($\sim$410 nm) where the reaction product (the *Z*-isomer) absorbs and an absorption decrease at the absorption bands of the educt molecules at higher wavelengths ($\sim$550 nm).

Details of the photochemical reaction dynamics can be obtained by modeling the absorption kinetics with exponential functions. The data are well fitted by the sum of three exponentials with time constants of 0.4, 2.2, and 7 ps used in combination with an additional offset. The amplitude spectra of the different components deduced from the global fitting analysis, the so-called decay associated spectra (DAS), are plotted in Figure 2c. The shape and the amplitudes of the DAS reveal information on the involved molecular processes: the DAS related to the subpicosecond process (Figure 2c, 0.4 ps) show the characteristics of a reaction on the excited-state potential energy surface. The weak change of the ESA together with a shift in the stimulated emission spectrum points to relaxation of the initially populated Franck−Condon state by

TABLE 1: Parameter for the Ring-Opening Reaction of the Investigated Indolylfulgide: Quantum Yields Obtained via Steady-State Experiments and Time Constants Determined by the Transient Absorption Experiments Evaluated by a Global Fitting Analysis

	stationary data		transient data			
process	$\lambda_{excitation}$ (nm)	QY (%)	$\lambda_{excitation}$ (nm)	τ_1 (ps) reorganization/S_N relaxation	τ_2 (ps) S_1 relaxation	τ_3 (ps) cooling
C→ *Z* (S_N)	365	28 ± 2	340	0.5	1.3	10
C→*Z* (S_1)	532	7 ± 1	570	0.4	2.2	7

Photochemistry in Fulgide Molecules

J. Phys. Chem. A, Vol. 112, No. 51, 2008 **13367**

Figure 2. (a/b) Transient absorption spectra (TS) at selected delay times for the two ring-opening reactions. (c/d) The right part shows decay associated spectra (DAS) derived from a global fitting routine.
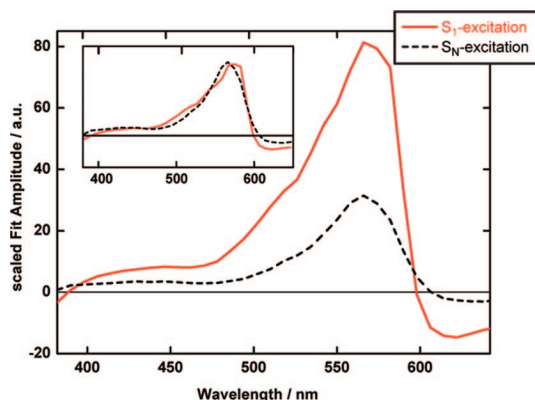
Figure 3. Comparison of the rescaled DAS spectra (see text) related to the time constants of 1.3 ps (black, broken, S_N excitation) and 2.2 ps (red, solid, S_1 excitation) for the decay of the S_1 state. The small amplitude observed after S_N excitation shows that only a small fraction (38%) of the molecules reaches the minimum of the S_1 state of the *C*-isomer. The inset spectra in the upper left are normalized to show the similarity of the two DAS spectra assigned to the S_1 decay.

wave packet motion, vibrational energy redistribution, and solvation processes with a time constant of 0.4 ps (Figure 2c, 0.4 ps). Subsequently, a dominant 2.2 ps process represents the decay of ESA and SE (Figure 2c, 2.2 ps). Its strong amplitude and the spectral shape indicate that the process is related to the transition into the electronic ground state ($S_1 \rightarrow S_0$, 2.2 ps). The dispersive shape of the weak 7 ps component exhibits the features expected from cooling processes of hot educt molecules in the electronic ground state (Figure 2c, 7 ps). Please note that the observed cooling behavior is a nonexponential process, which can only be described qualitatively by the fit procedure. The time constant of 7 ps may hence be seen as an approximate value for the kinetics of the cooling process. These absorbance changes are related to molecules which do not undergo the ring-opening reaction but return to the educt state with considerable excess energy. From the weak amplitude of the long-lasting absorption change (Figure 2c, offset), one can deduce that only

a small percentage of the originally excited *C*-isomers have completed the ring-opening reaction. This observation is in agreement with the small quantum yield of 7% observed upon steady-state excitation of the S_1 state.

C→*Z* **Reaction via S_N Excitation.** The transient spectra obtained after excitation in the ultraviolet ($\lambda_{exc} = 340$ nm) are depicted in Figure 2b. At first glance, the results differ significantly from the ones obtained after visible excitation (Figure 2a and c). Excitation to the S_N state leads to a broad instantaneous absorption increase (because of excited-state absorption) within the investigated spectral range ($t_D = 0.2$ ps, Figure 2b). This early ESA shows pronounced modulations at 530 and 650 nm. On the time scale of several 100 fs, these ESA signals start to decrease while an absorption peak appears at 580 nm (Figure 2c, $t_D = 0.2$ ps, 0.5 ps). The ESA signal decays on the time scale of 1−2 ps (Figure 2c, $t_D = 0.5$, 1, and 2 ps). During this time, a net absorption decrease appears in the wavelength range where the ground state of the original *C*-form absorbs (Figure 2c, $t_D = 2$ ps, 5 ps). On the 10 ps time scale, some weak residual transients lead to the final constant absorption change. This offset represents the disappearance of the original *C*-form (at long wavelengths 460−620 nm) and the formation of the *Z*-form (at short wavelengths <460 nm).

When modeling the experimental data with multiexponential kinetics, a reasonable quality of the fit is found for three exponentials with time constants of 0.5, 1.3, and 10 ps together with a final offset (Figure 2d). Modeling the data with more than three kinetic components did not lead to any significant improvement of the quality of the fit. It will be shown later why the same number of time constants and intermediates is found for both S_1 and S_N excitation (Figure 2b and d).

The investigation of the DAS reveals a qualitative similarity of the data obtained for both excitation conditions concerning the slower reaction dynamics >1 ps. The final absorption change at delay times >50 ps has identical spectral shape for both excitations. However, the amplitudes are very different for the two situations: in the case of S_N excitation, the amplitude is
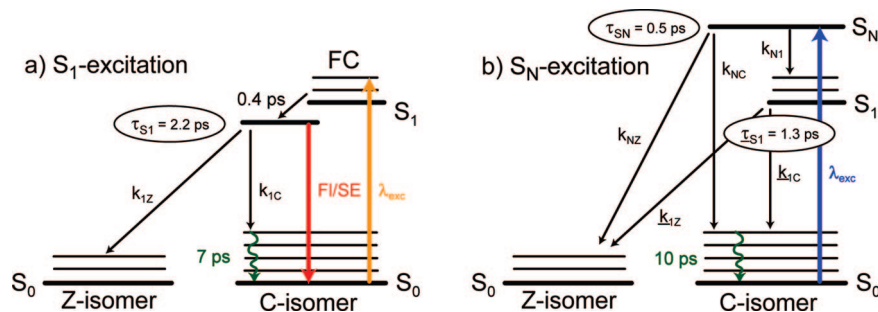
Figure 4. State models for the different photochemical reaction pathways after excitation into the S_1 and S_N bands. Panel a shows the suggested reaction scheme after visible excitation while panel b describes higher excitation using UV light.

about 4 times larger than that upon S_1 excitation. The spectral shape of the 10 ps kinetic component (Figure 2d, S_N excitation) also resembles the one of the 7 ps component (Figure 2b, S_1 excitation). Both may therefore be assigned to cooling dynamics of reformed educt molecules in the electronic ground state. The DAS for the S_1 decay have a similar spectral shape. However, their amplitudes differ strongly. This is demonstrated by the normalized DAS of these components shown as the insert in Figure 3 (upper left). The pronounced similarity of the DAS for the picosecond kinetic components indicates that both excitation conditions lead to the population and subsequent decay of the S_1 state.

As expected from qualitative considerations, the subpicosecond behavior of the two samples differs strongly. The 0.5 ps DAS observed upon S_N excitation reflect features related to the decay of the S_N state and to the formation of the S_1 state. We find the decay of absorption peaks at 550 and 650 nm associated with ESA from the S_N state and the formation of the 580 nm ESA peak of the S_1 state together with the stimulated emission of the S_1 state.

For a more quantitative treatment of the reaction dynamics, we have to refer to the amplitudes of the DAS for the two excitation conditions. To avoid the uncertainties related to the absolute determination of pump intensities and the spatial overlap between pump and probe pulses in the two experiments, we rescale the DAS using the amplitudes of the final offset spectra found in the two transient experiments. This offset represents the absorbance change due to the formation of the Z-isomer. Since the quantum yield for S_N excitation is 4 times larger than for S_1 excitation (Table 1), the rescaled offset spectrum for S_N excitation should have 4 times the amplitude of that spectrum observed upon S_1 excitation. A scaling factor of 0.98 for the S_1 excited data is found. The DAS of the S_1 decay plotted in Figure 3 with rescaled amplitudes show that the relative amplitude of the 1.3 ps DAS, which represents the decay of the transiently formed S_1 state after S_N excitation, is considerably smaller (factor 0.38) than the corresponding 2.2 ps DAS amplitude observed upon S_1 excitation. This gives strong indications that after S_N excitation a considerable fraction of the molecules do not react via the S_1 state or pass through it only transiently. A more detailed analysis will be presented below.

Discussion

Reaction Scheme for the Ring-Opening Reaction after S_1 Excitation. Related indolylfulgides and indolylfulgimides have been recently investigated with different time-resolved methods.[28−31] Following the model for the ring-opening reaction proposed in ref 29, we will now assign the observed transient signals to distinct reaction steps (see Figure 4a): using 570 nm light, the

molecules are excited into the Franck−Condon region (FC). The initial absorption increase represents a strong ESA with a pronounced peak at 580 nm. SE is found in the wavelength range above 600 nm. From the FC region, the molecules undergo fast vibrational wave packet motion, vibrational relaxation, and solvent rearrangement processes on the time scale of a few 100 fs (Figure 4a). These processes give rise to a subpicosecond (0.4 ps) kinetic component. On the time scale of 1 ps, the absorption spectrum still shows the ESA features, which are characteristic for the population of the S_1 state. The photochemical reaction itself (Figure 2a and c) is associated with the decay of the excited state showing the time constant $\tau_{S1} = 2.2$ ps (Figure 4a). Its DAS display the signatures of vanishing ESA and reformation of ground-state absorption of the C- and the Z-isomer. The final kinetic component with a time constant of 7 ps has a weak amplitude with a dispersive shape: absorption decreases at longer wavelengths (>570 nm) and increases at shorter wavelengths. These spectral signatures are characteristic for cooling of a hot fulgide in its C-form.[29] This feature originates from the fraction of excited molecules, which do not undergo the ring-opening reaction (>90%) but relax via internal conversion into a "hot" C-ground state (Figure 4a). After the cooling process, the photoreaction itself and all photophysical processes are completed. The offset spectrum reached at late delay times $t_D > 50$ ps reproduces the stationary difference spectrum between Z- and C-isomer absorption (see Figure 1): additional absorption appears around 420 nm because of photoproduct formation (Z) and absorption reduction is detected between 500 and 650 nm because of the disappearance of the educt (C). The essential photochemical reaction occurs from the relaxed S_1 state where the reaction branches (Figure 4a) into the photochemical active process (7%, rate k_{1Z}) and internal conversion (93%, rate k_{1C}). These two rates combine to the observed decay rate $k_{S1} = 1/\tau_{S1} = k_{1Z} + k_{1C}$. The radiative rate constants can be neglected because of its small value. Measurements of the temperature dependence of the quantum yield and the reaction dynamics of fulgides have shown that both processes are thermally activated with a larger barrier for the photochemical pathway.[32−34]

Ring-Opening after S_N Excitation. In Figure 4b, the schematic model for the reaction dynamics observed after S_N excitation is shown. Optical excitation at 340 nm populates the S_N state. The S_N state is left within 0.5 ps, and molecules with spectral signatures of the S_1 state are observed (Figure 4b). The subsequent decay of the S_1 state occurs with the time constant $\tau_{S1} = 1.3$ ps. The faster time constant for the decay of the S_1 state observed after S_N excitation (1.3 ps versus 2.2 ps for S_1 excitation) may be explained as follows: relaxation from the S_N state populates the S_1 state with vibrational excess energy. This increased vibrational excitation may lead to an accelerated

Photochemistry in Fulgide Molecules

J. Phys. Chem. A, Vol. 112, No. 51, 2008 **13369**

TABLE 2: Characteristic Parameters for the Ring-Opening Reaction after Excitation at 340 nm (Higher Excited Electronic State S_N)[a]

	case 1: QY $(S_1 \rightarrow Z) = 7\%$	case 2: constant k_{1C}
ring-opening from S_1: $\underline{k}_{1Z}/ps^{-1}$	0.054	0.347
internal conversion from S_1: $\underline{k}_{1C}/ps^{-1}$	0.715	0.423
reaction from S_N: k_{N1}/ps^{-1}	0.76	0.76
k_{NZ}/ps^{-1}	0.507	0.218
k_{NC}/ps^{-1}	0.733	1.022
$\underline{QY}(S_1 \rightarrow Z)$	7%	45%
QY via S_1	2.7%	17%
$QY_{direct}(S_N \rightarrow Z)$	25.3%	11%

[a] Two situations are calculated where different models for the reaction out of the hot state S_1 are assumed: Case 1 assumes that the quantum yield from state S_1 is constant, and case 2 assumes a constant internal conversion k_{1C} out of the S_1 state.
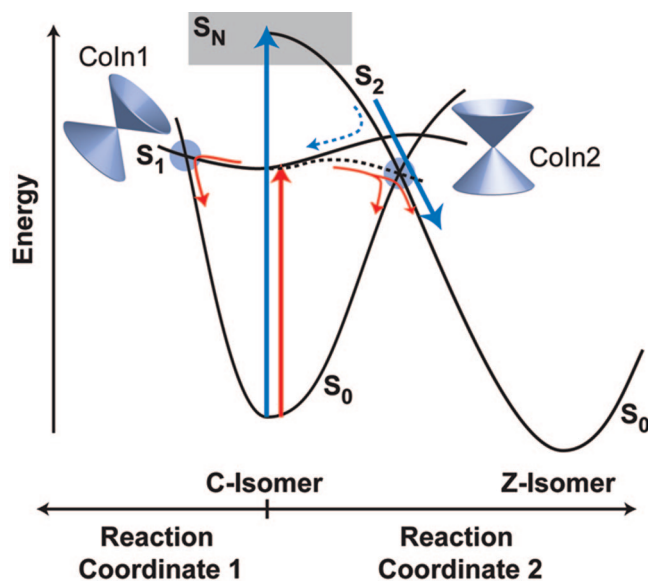
Figure 5. Suggested potential energy surfaces for the photochemical ring-opening reaction of the investigated indolylfulgide starting after excitation into the S_1 (red arrow) and the S_N (blue) state.

reaction out of S_1 (in the case of thermally activated decay channels[32]). The acceleration of the S_1 decay after S_N excitation $\underline{\tau}_{s1} > \underline{\tau}_{s1}$ is considered by the new decay rates $\underline{k}_{1Z}$ and $\underline{k}_{1C}$ used instead of the rates k_{1Z} and k_{1C} describing the decay of the S_1 state after direct optical excitation (see Figure 4a). For a complete population transfer from S_N to S_1, the amplitude of the 1.3 ps DAS would be expected to be similar to the amplitude of the 2.2 ps DAS after S_1 excitation. However, as shown above, the relative amplitude of the 1.3 ps kinetic component is strongly reduced to 38% (see Figure 3) compared to the one of the 2.2 ps component. This reduction indicates that the excited electronic state S_1 is only formed for 38% of all fulgide molecules originally excited into the S_N state. The remaining population (62%) of the molecules follows a different reaction pathway out of the S_N state. This additional reaction path needs further considerations (Figure 4b).

The scheme in Figure 4b considers the different potential reaction channels originating from the state S_N. The rate k_{N1} describes internal conversion to the S_1 state, k_{NC} is the direct conversion to the ground state of the C-isomer, and k_{NZ} is related to the direct ring-opening reaction without the involvement of

the S_1 state (Figure 4b). The S_N state decays with the experimentally observed time constant $\tau_{SN} = 0.5$ ps. This time constant is related to the three decay rates:

$$\frac{1}{\tau_{SN}} = k_{SN} = k_{N1} + k_{NZ} + k_{NC} \quad (1)$$

The rate constant k_{N1} for the transfer to the first excited-state S_1 can directly be determined from the measured time constant $\tau_{SN} = 0.5$ ps and the quantum yield $QY(S_N \rightarrow S_1) = 0.38$ for the formation of the S_1 state.

$$QY(S_N \rightarrow S_1) = k_{N1}/k_{SN}; \ k_{N1} = 0.76 ps^{-1} \quad (2)$$

The value of $k_{N1} = 0.76$ ps^{-1} corresponds to a time constant of $\tau_{N1} = 1.3$ ps for internal conversion from $S_N \rightarrow S_1$, which is surprisingly slow compared to relaxational processes from $S_N \rightarrow S_1$ found in other molecules.[35]

It is of special interest whether the photochemical ring-opening reaction after S_N excitation still occurs via the S_1 state or directly from the excited S_N state (rate k_{NZ}). In general, this question can be addressed by an analysis of the experimental results. Unfortunately, the very large amplitudes related to the ESA dynamics and the weak changes in ground-state absorption upon ring-opening do not allow to determine the yield for direct product formation out of S_N from the recorded absorption spectra without further assumptions. However, the question may be handled with additional information on the efficiency of the ring-opening reaction out of the "hot" S_1 state. The total quantum yield for the ring-opening reaction (Z-isomer formation) is the sum of the contributions from the direct ring-opening reaction $QY_{direct}(S_N \rightarrow Z)$ and the reaction via S_1:

$$QY_{total}(S_N \rightarrow Z) = QY_{direct}(S_N \rightarrow Z) + QY_{indirect}(S_N \rightarrow Z) =$$
$$QY_{direct}(S_N \rightarrow Z) + QY(S_N \rightarrow S_1) \cdot \underline{QY}(S_1 \rightarrow Z) =$$
$$\frac{k_{NZ}}{k_{N1} + k_{NZ} + k_{NC}} + \frac{k_{N1}}{k_{SN}} \cdot \frac{\underline{k}_{1Z}}{\underline{k}_{1Z} + \underline{k}_{1C}} = \frac{k_{NZ}}{k_{SN}} + \frac{k_{N1}}{k_{SN}} \cdot \frac{\underline{k}_{1Z}}{\underline{k}_{S1}} \quad (3)$$

The quantities $k_{SN} = 2.0$ ps^{-1} and $\underline{k}_{S1} = 1/\underline{\tau}_{S1} = 0.76$ ps^{-1} and the quantum yield $QY_{total}(S_N \rightarrow Z) = 0.28$ are directly measured. The rate $k_{N1} = 0.76$ ps^{-1} is obtained above in eq 2. Information on the value $\underline{k}_{1Z}$ would allow calculations of the value k_{NZ} for the direct ring-opening out of S_N. On the basis of the experimental results, we may calculate values for the reaction rate k_{NZ} (Table 2) and for the yield of the different reaction channels under certain limiting assumptions on the ring-opening reaction.

Case 1. It is assumed that the quantum yield for ring-opening out of the hot S_1 state, $\underline{QY}(S_1 \rightarrow Z)$, does not depend on the preparation of state S_1 and stays at $\underline{QY}(S_1 \rightarrow Z) = QY(S_1 \rightarrow Z) = 0.07$ known from steady-state experiments. In this special case, the evaluation of eq 3 reveals that the ring-opening reaction proceeds predominantly via the direct reaction channel. The direct rate $k_{NZ} = 0.507$ ps^{-1} is ultrafast, and only 2.7% of the excited molecules react via the S_1 state to the Z-isomer (Table 2). The rest of the ring-opening reaction (25.3%) proceeds directly from S_N (Table 2).

Case 2. This case treats the extreme situation where we assume that the decreased S_1 lifetime observed after S_N excitation (from 2.2 to 1.3 ps) is only caused by an increase in the reaction rate $\underline{k}_{1Z}$ because of the hot S_1 state while the internal conversion rate stays constant, $\underline{k}_{1C} = k_{1C}$. Eq 3 shows that $\underline{k}_{1Z}$ would increase from a value of 0.054 ps^{-1} to 0.343 ps^{-1} in this case (Table 2). Under these conditions, the quantum yield $\underline{QY}(S_1 \rightarrow Z)$ would be close to 45% (instead of 7% in the original
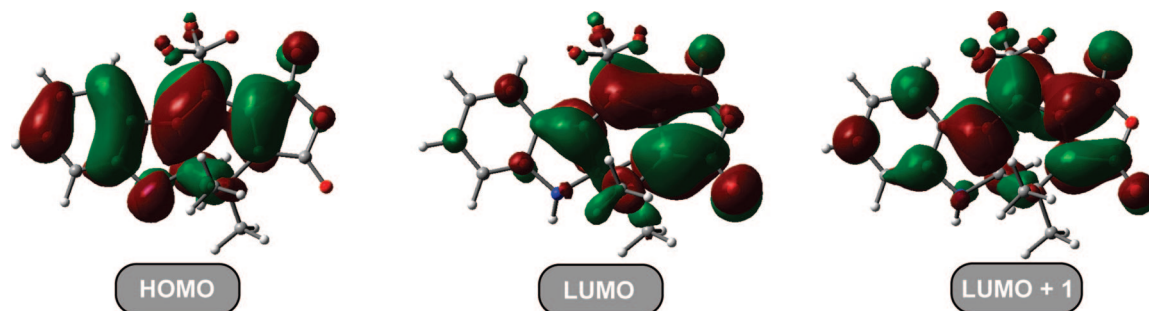
Figure 6. CASSCF frontier orbitals contributing to the electronic wave functions of S_0, S_1, and S_2.

case), and 17% of the excited molecules would react via the S_1 channel (Table 2). However, even in this unrealistic case, a significant fraction (ca. 11%) would follow the direct reaction path from the S_N state.

In a realistic situation, the efficiency for the direct ring-opening reaction channel will be somewhere between 11% and 28%. Independent of the model assumptions, however, is the experimental facts that (1) only 38% of the excited S_N molecules remain trapped transiently in the S_1 state and that (2) the transfer rate from S_N to S_1 of $k_{N1} = 0.76$ ps^{-1} is unusually small. This attributes a greater importance to other reaction channels which do not lead to the S_1 state of the *C*-isomer, which may be represented by a new rate constant $k_{other} = k_{SN} - k_{N1} = 1.24$ ps^{-1}. The reduced population of the S_1 state (38%) resulting from the small value of k_{N1} is in contradiction to the assumptions leading to Kasha's rule. In our case, the deviation from Kasha's rule is not observed via the emission properties of the sample but in terms of a strongly modified photochemical reaction.

To explain the experimental observations, a schematic view of the potential energy surfaces is shown in Figure 5: excitation of the *C*-isomer with visible light (Figure 5, red arrows) populates the excited electronic state S_1. From here, the molecules may return to the ground state via two different pathways. Both reaction channels are thermally activated with different barrier heights. This idea is well supported by theoretical findings. On the level of CASSCF(6,6) calculations using full-state average-corrected gradients, two conical intersections between S_1 and S_0 (CoIn1 and CoIn2, see Figure 5 and Supporting Information) could be located in a region reachable from the FC-transition of the *C*-isomer. They show a distinct different topology; for details, see Supporting Information. CoIn1 is tilted in a way that allows only back transfer to the *C*-isomer. Accordingly, the geometry of CoIn1 is similar to the geometry of the *C*-isomer. The second conical intersection (CoIn2) lies 0.26 eV below the first one; its structure is between the equilibrium geometries of both isomers, and its peaked topology opens both reaction channels to the *Z*- as well as to the *C*-isomer.

Optical excitation in the manifold of the S_N state may lead to a motion toward the crossing of the S_2 and S_1 surfaces. A first branching occurs (Figure 5 blue solid and broken arrows) where ~40% of the molecules pass to the minimum of the S_1 surface, while ~60% continue on the diabatic path and quickly reach the conical intersection CoIn2. Here, the final branching into the ring-opened or -closed form may occur. The fraction of molecules trapped in the S_1 state of the *C*-isomer will further react as described above for direct S_1 exciation (Figure 5, red arrows).

The question remains why only ~40% of the molecules excited to the S_N state arrive in the S_1 state. Our results presented

above suggest that the coupling between the higher excited electronic state S_N and the first excited-state S_1 should be rather weak. An explanation can be found in the electronic wave functions. Figure 6 shows a comparison of the frontier orbitals contributing to the electronic wave functions of ground and excited states. From the highest occupied molecular orbital (HOMO) to the lowest unoccupied molecular orbital (LUMO), the antibonding character of the π-bonds increases in the central C6-ring and its σ-bond is softened. For the S_2 state, contributions from the doubly occupied LUMO become dominant. This configuration correlates directly with the ground-state configuration of the *Z*-form. This may accelerate the direct ring-opening reaction and may also lead to a small rate of internal conversion from S_N to S_1.

Conclusions

The present study shows that after S_1 excitation (Scheme 1) the ring-opening reaction of the investigated fluorinated indolylfulgide follows the already published reaction scheme.[31] The reaction quantum yield for the S_1 induced process is only moderate in the range of ~7%. Excitation of the *C*-isomer with light at 340 nm results in the population of a higher excited electronic state S_N with an unexpected long lifetime of 0.5 ps. During the relaxation of this state, only ~40% of the excited molecules are transferred to the minimum of the first excited electronic state S_1. These experimental results are in contradiction to the assumptions of Kasha's rule where higher electronic states S_N should decay exclusively via internal conversion to the lowest excited state. However, in the case of the studied indolylfulgide, the majority of excited molecules undergoes direct internal conversion to the ground state of the *C*-isomer or direct photoreaction to the *Z*-isomer. This manifests itself in an increase of the photochemical quantum yield to ~30% for S_N excitation compared to ~7% for S_1 excitation. Results and interpretations are confirmed by quantum-chemical calculations.

Supporting Information Available: Details and further results of the quantum-chemical calculations. This material is available free of charge via the Internet at http://pubs.acs.org.

References and Notes

(1) Kasha, M. *Discuss. Faraday Soc.* **1950**, 14–19.
(2) Turro, N. J.; Ramamurthy, V.; Cherry, W.; Farneth, W. *Chem. Rev.* **1978**, *78*, 125–145.

Photochemistry in Fulgide Molecules

J. Phys. Chem. A, Vol. 112, No. 51, 2008 **13371**

(3) Zimmerman, H. E.; Wilson, J. W. *J. Am. Chem. Soc.* **1964**, *86*, 4036–4042.

(4) Englman, R.; Jortner, J. *Mol. Phys.* **1970**, *18*, 145–164.

(5) Birks, J. B. *Organic molecular photophysics*; John Wiley and Sons Ltd.: New York, 1973; Vol. *I*, p 32.

(6) Bearpark, M. J.; Bernardi, F.; Clifford, S.; Olivucci, M.; Robb, M. A.; Smith, B. R.; Vreven, T. *J. Am. Chem. Soc.* **1996**, *118*, 169–175.

(7) Levine, S. Z.; Knight, A. R.; Steer, R. P. *Chem. Phys. Lett.* **1974**, *29*, 73–76.

(8) Oka, T.; Knight, A. R.; Steer, R. P. *J. Chem. Phys.* **1977**, *66*, 699–706.

(9) Binsch, G.; Hexlbronner, E.; Jankow, R.; Schmidt, D. *Chem. Phys. Lett.* **1967**, *1*, 135–138.

(10) Beer, M.; Longuethiggins, H. C. *J. Chem. Phys.* **1955**, *23*, 1390–1391.

(11) Fujino, T.; Yu, S.; Tahara, T. *Bull. Chem. Soc. Jpn.* **2002**, *75*, 1031–1040.

(12) (a) Murakami, M.; Miyasaka, H.; Okada, T.; Kobatake, S.; Irie, M. *J. Am. Chem. Soc.* **2004**, *126*, 14764–14772. (b) Ishibashi, Y.; Murakami, M.; Miyasaka, H.; Kobatake, S.; Irie, M.; Yokoyama, Y. *J. Phys. Chem. C* **2007**, *111*, 2730–2737.

(13) Birks, J. B. *Chem. Phys. Lett.* **1972**, *17*, 370–372.

(14) Wurzer, A. J.; Wilhelm, T.; Piel, J.; Riedle, E. *Chem. Phys. Lett.* **1999**, *299*, 296–302.

(15) Diau, E. W. G.; De Feyter, S.; Zewail, A. H. *J. Chem. Phys.* **1999**, *110*, 9785–9788.

(16) Wolak, M. A.; Gillespie, N. B.; Thomas, C. J.; Birge, R. R.; Lees, W. J. *J. Photochem. Photobiol., A: Chem.* **2001**, *144*, 83–91.

(17) Cordes, T.; Weinrich, D.; Kempa, S.; Riesselmann, K.; Herre, S.; Hoppmann, C.; Rück-Braun, K.; Zinth, W. *Chem. Phys. Lett.* **2006**, *428*, 167–173.

(18) Spörlein, S.; Carstens, H.; Satzger, H.; Renner, C.; Behrendt, R.; Moroder, L.; Tavan, P.; Zinth, W.; Wachtveitl, J. *Proc. Natl. Acad. Sci. U.S.A.* **2002**, *99*, 7998–8002.

(19) Cordes, T.; Heinz, B.; Regner, N.; Hoppmann, C.; Schrader, T. E.; Summerer, W.; Rück-Braun, K.; Zinth, W. *ChemPhysChem* **2007**, *8*, 1713–1721.

(20) Cordes, T.; Schadendorf, T.; Priewisch, B.; Rück-Braun, K.; Zinth, W. *J. Phys. Chem. A* **2008**, *112*, 581–588.

(21) Wilhelm, T.; Piel, J.; Riedle, E. *Opt. Lett.* **1997**, *22*, 1494–1496.

(22) Riedle, E.; Beutter, M.; Lochbrunner, S.; Piel, J.; Schenkl, S.; Sporlein, S.; Zinth, W. *Appl. Phys. B: Lasers Opt.* **2000**, *71*, 457–465.

(23) Huber, R.; Satzger, H.; Zinth, W.; Wachtveitl, J. *Opt. Commun.* **2001**, *194*, 443–448.

(24) Seel, M.; Wildermuth, E.; Zinth, W. *Meas. Sci. Technol.* **1997**, *8*, 449–452.

(25) Satzger, H.; Zinth, W. *Chem. Phys.* **2003**, *295*, 287–295.

(26) Frisch, M. J.; Trucks, G. W.; Schlegel, H. B.; Scuseria, G. E.; Robb, M. A.; Cheeseman, J. R.; Montgomery, J. A., Jr.; Vreven, T.; Kudin, K. N.; Burant, J. C.; Millam, J. M.; Iyengar, S. S.; Tomasi, J.; Barone, V.; Mennucci, B.; Cossi, M.; Scalmani, G.; Rega, N.; Petersson, G. A.; Nakatsuji, H.; Hada, M.; Ehara, M.; Toyota, K.; Fukuda, R.; Hasegawa, J.; Ishida, M.; Nakajima, T.; Honda, Y.; Kitao, O.; Nakai, H.; Klene, M.; Li, X.; Knox, J. E.; Hratchian, H. P.; Cross, J. B.; Bakken, V.; Adamo, C.; Jaramillo, J.; Gomperts, R.; Stratmann, R. E.; Yazyev, O.; Austin, A. J.; Cammi, R.; Pomelli, C.; Ochterski, J. W.; Ayala, P. Y.; Morokuma, K.; Voth, G. A.; Salvador, P.; Dannenberg, J. J.; Zakrzewski, V. G.; Dapprich, S.; Daniels, A. D.; Strain, M. C.; Farkas, O.; Malick, D. K.; Rabuck, A. D.; Raghavachari, K.; Foresman, J. B.; Ortiz, J. V.; Cui, Q.; Baboul, A. G.; Clifford, S.; Cioslowski, J.; Stefanov, B. B.; Liu, G.; Liashenko, A.; Piskorz, P.; Komaromi, I.; Martin, R. L.; Fox, D. J.; Keith, T.; Al-Laham, M. A.; Peng, C. Y.; Nanayakkara, A.; Challacombe, M.; Gill, P. M. W.; Johnson, B.; Chen, W.; Wong, M. W.; Gonzalez, C.; Pople, J. A. *Gaussian 03*, revision C.02; Gaussian, Inc.: Wallingford, CT, 2004.

(27) Yokoyama, Y. *Chem. Rev.* **2000**, *100*, 1717–1739.

(28) Koller, F. O.; Schreier, W. J.; Schrader, T. E.; Sieg, A.; Malkmus, S.; Schulz, C.; Dietrich, S.; Ruck-Braun, K.; Zinth, W.; Braun, M. *J. Phys. Chem. A* **2006**, *110*, 12769–12776.

(29) Malkmus, S.; Koller, F. O.; Heinz, B.; Schreier, W. J.; Schrader, T. E.; Zinth, W.; Schulz, C.; Dietrich, S.; Rück-Braun, K.; Braun, M. *Chem. Phys. Lett.* **2006**, *417*, 266–271.

(30) Heinz, B.; Malkmus, S.; Laimgruber, S.; Dietrich, S.; Schulz, C.; Rück-Braun, K.; Braun, M.; Zinth, W.; Gilch, P. *J. Am. Chem. Soc.* **2007**, *129*, 8577–8584.

(31) Malkmus, S.; Koller, F. O.; Draxler, S.; Schrader, T. E.; Schreier, W. J.; Brust, T.; DiGirolamo, J. A.; Lees, W. J.; Zinth, W.; Braun, M. *Adv. Funct. Mater.* **2007**, *17*, 3657–3662.

(32) Brust, T.; Draxler, S.; Malkmus, S.; Schulz, C.; Zastrow, M.; Rück-Braun, K.; Zinth, W.; Braun, M. *J. Mol. Liq.* **2008**, doi: 10.1016/j.molliq. 2008.02.011.

(33) Heller, H. G. *Spec. Publ.−R. Soc. Chem.* **1986**, *60*, 120–135.

(34) Matsui, F.; Taniguchi, H.; Yokoyama, Y.; Sugiyama, K.; Kurita, Y. *Chem. Lett.* **1994**, 1869–1872.

(35) Shank, C. V.; Ippen, E. P.; Teschke, O. *Chem. Phys. Lett.* **1977**, *45*, 291–294.